IEEE Access
Multidisciplinary | Rapid Review | Open Access Journal

Received April 13, 2020, accepted April 28, 2020, date of publication May 11, 2020, date of current version May 21, 2020.

Digital Object Identifier 10.1109/ACCESS.2020.2993692

Stator Single-Line-to-Ground Fault Protection for Bus-Connected Powerformers Based on S-Transform and Bagging Ensemble Learning

YUANYUAN WANG, (Member, IEEE), YONGSHENG GUO, XIANGJUN ZENG, (Senior Member, IEEE), JUN CHEN, YANG KONG, AND SHANFENG SUN

School of Electrical and Information Engineering, Changsha University of Science and Technology, Changsha 410114, China

Corresponding author: Yuanyuan Wang (wyy_1202@163.com)

This work was supported in part by the National Natural Science Foundation of China under Grant 51777014, in part by the Hunan Provincial Key Research and Development Program under Grant 2018GK2057, in part by the Educational Commission of Hunan Province of China under Grant 18A124, in part by the Changsha Science and Technology Project under Grant kq1901104, and in part by the Hunan Graduate Research and Innovation Project under Grant CX20190686 and Grant CX2018B556.

ABSTRACT In order to achieve selective ground fault protection for bus-connected Powerformers and improve the reliability of the protection scheme, this paper presents a novel stator single-line-to-ground (SLG) fault protection scheme for bus-connected Powerformers based on S-transform (ST) and bagging ensemble learning algorithm. The scheme utilizes ST to decompose the zero-sequence current signals acquired from the Powerformer terminal to obtain the amplitude-time-frequency matrix. Then, fault features extraction is presented, and three features including the transient energy, the comprehensive correlation coefficient, and the zero-sequence active power are discussed and selected as feature vectors. The calculated data set is then extracted from feature vectors and used as inputs to the bagging ensemble learning algorithm to detect faults. Simulation results have shown that, under different fault conditions, the novel scheme can detect in which Powerformer a stator SLG fault is occurring and can detect internal faults from external faults reliably even if the fault resistance is at 8000 Ω. The proposed protection scheme does not need to set the threshold value and has noise-tolerant ability. Furthermore, the proposed technique performs better than support vector machine (SVM), random forest (RF) and k-Nearest Neighbor (KNN) techniques in detecting faults.

INDEX TERMS Powerformer, protection scheme, stator single-line-to-ground fault, S-transform, bagging ensemble learning.

I. INTRODUCTION

Electric utilities are increasingly being asked to minimize blackouts as most of economic losses of the customer due to longer period of interruptions caused by faults. In this context, the development of fast and reliable power system fault protection technology is a problem that has been extensively studied for decades in the world.

The SLG fault is the most frequent of many fault types, which seriously affects the operating state of the power equipment and the stability of the power grid, so this paper makes an in-depth study of SLG fault. Particularly, when a SLG fault occurs on the stator winding of Powerformer (high terminal voltage generator, in theory, up to 400kV), the fault tends to develop into more severe turn-to-turn faults or phase-to-phase faults, and even lead to cable explosion and Powerformer damage, thereby reduces the reliability of the grid power supply and cause huge economic losses. Therefore, it is of great significance to study the stator SLG fault protection of Powerformer.

Nowadays, many protection schemes only for stator SLG fault for conventional generator have been developed. The zero-sequence fundamental over-voltage relay has blind zones near the generator neutral, so it can only be used to determine the fault at the generator terminal [1], [2]. The sub-harmonic voltage injection scheme with neutral grounding signal [3] and the third-harmonic voltage scheme [4] are important schemes to solve the blind zones. But the

The associate editor coordinating the review of this manuscript and approving it for publication was Mehdi Savaghebi.

former requires additional sub-harmonic power supplies, which increases the investment costs for the implementation of protection, while the latter achieves certain applications. Reference [5] proposed an adaptive stator SLG fault protection scheme based on third-harmonic differential voltage, which can realize the identification of stator SLG fault of generator and cover 100% of the stator windings. However, the protection based on the voltage signal cannot achieve selective protection, because each generator that is connected in parallel with the faulty generator has the same voltage.

In electric power plants, multiple Powerformers are connected to the same bus in parallel. If a stator SLG fault occurs in one of the bus-connected Powerformers, the protection scheme should detect in which Powerformer the ground fault is occurring. In order to solve this problem for bus-connected Powerformers, many protection schemes for stator SLG fault have been proposed and applied. Novel criterions were proposed in [6], which based on the direction of leakage currents, the magnitude of leakage currents, and the fault point energy dissipation, respectively. However, these independent protection schemes use only one fault feature as a criterion, and their reliability is low. On the basis of [6], in order to fuse as much fault features as possible to improve the reliability of the protection scheme, [7] and [8] further proposed protection schemes of the stator SLG fault for Powerformer based on hierarchical clustering and fuzzy clustering, respectively. The magnitude and direction of the zero-sequence current, the magnitude and direction of the leakage current are extracted as fault features and are used as inputs to the classification model. The reliability of the protection schemes has improved, but above-mentioned protection schemes have not verified the protection accuracy with measurement noises. A reliable solution for stator SLG fault protection for bus-connected Powerformer with selectivity has still not been found.

Nowadays, some classic single machine learning algorithms have achieved good results in fault detection, diagnosis and protection of power system, such as SVM [9], RF [10], KNN [11]. If these methods are applied to generator protection, it is expected to improve the performance of generator protection. However, the use of a single method may lead to poor generalization performance due to randomness and interference [12]. Fortunately, [13] and [14] have shown that the ensemble learning classification technique has advantages over single algorithm in improving the accuracy of fault protection and enhancing anti-interference ability. In order to improve the fault protection accuracy under unfavorable conditions (with noise, via high fault resistance), a fault protection technology based on ensemble learning classifier (bagging [15]) is proposed in this paper. With the help of bagging, three base classifiers of SVM, RF, and KNN are trained for different sampling subsets. Then the results of each basic classifier are voted to obtain a strong classifier to maximize the accuracy of the stator SLG fault protection for Powerformer.

In this paper, a novel stator SLG fault protection scheme for Powerformer based on ST and bagging ensemble learning algorithm is proposed. The main contributions of the paper are as follows:

(1) The fault features generated by Powerformer is non-stationary. We find that ST is more suitable for Powerformer fault feature extraction than the Short-time Fourier Transform (STFT) with fixed window width and the Wavelet Transform (WT) with mother wavelet to be selected. In this paper, ST is used to decompose the non-stationary fault signals including the phase information and the absolutely-referenced frequency information in full time-frequency range, which can extract fault features more effectively.

(2) Powerformer protection is to judge whether the equipment is faulty or not, which can be regarded as a classification problem. Among the existing classification algorithms, ensemble learning algorithms can improve the accuracy of fault classification, among which bagging is a well-known representative of ensemble learning algorithms. Bagging can train different sample subsets with the given base classifiers, and then vote the results of each base classifier to get a strong classifier. This paper uses the bagging ensemble learning algorithm for fault identification to improve the performance of the protection scheme. In addition, the classification technology of bagging ensemble learning is based on the difference of feature vectors, so the proposed protection scheme does not need to set threshold.

(3) When the fault resistance reaches 5000 Ω, the fault detection accuracy of general protection schemes is low. While the proposed protection scheme can correctly identify the fault with a fault resistance of 8000 Ω.

(4) The proposed technique shows better generalization ability and noise-tolerant ability than SVM, RF and KNN techniques in detecting faults.

This paper is organized as follows: In Section II, the principle of ST and bagging ensemble learning algorithm are introduced. In Section III, the fault features of stator SLG fault for Powerformer are analyzed, and the extraction process of the feature vectors is introduced. Next, in Section IV, the protection principle of stator SLG fault for Powerformers is proposed. Simulation experiments to verify the proposed scheme are shown in Section V, and the conclusions are given in Section VI.

II. BACKGROUND THEORIES

A. S-TRANSFORM

The fault information extracted from the stator SLG fault is generally a non-stationary signal, which requires signal processing techniques to transform the measured data into a more informative analysis domain to reveal the hidden features of the fault. Fourier Transform (FT) and Fast Fourier Transform (FFT) are the first generation of signal processing tools, which can effectively analyze stationary signals, but when processing non-stationary signals, error information will be generated due to the loss of time data. In response

to this, STFT decomposes the entire time-domain process into multiple small processes (windows) of equal width. Each small process is approximately stationary, and then FT can be used to capture the change of signal frequency with time. But for time-varying, non-stationary signals, the high frequency is suitable for narrow windows while the low frequency is suitable for wide windows. However, the window of STFT is fixed, so the STFT still cannot capture the change of frequency of time-varying signal with time. After that, Wavelet Transform (WT) appears, it inherits and develops the idea of STFT signal analysis and processing, and overcomes the shortcoming that the window width does not change with frequency. It is an ideal tool for signal time-frequency analysis and processing. However, WT-based fault detection technology also has the following disadvantages: (1) Narrow high-frequency support range; (2) Subjective choice of mother wavelet; (3) Lack of feature resolution [16].

ST can solve aforementioned shortcomings and deal with non-stationary signals [17]. It introduces a Gaussian window function whose window width changes with frequency, so as to obtain a time-frequency matrix corresponding to the frequency. It has the advantages of linearity, locality, lossless reversibility and good time-frequency resolution. Therefore, this paper utilizes ST to extract the fault features.

ST is developed by the STFT of the normalized Gaussian window and the phase-corrected WT. The ST of a time signal $x(t)$ is defined as:

$$S(\tau, f) = \int_{-\infty}^{\infty} x(t) w(t-\tau, f) e^{-j2\pi ft} dt \tag{1}$$

$$w(t-\tau, f) = \frac{|f|}{\sqrt{2\pi}} e^{\frac{-f^2(t-\tau)^2}{2}} \tag{2}$$

where $w(t-\tau, f)$ is the Gaussian window, τ and f are the transform time and frequency coordinates, and j is the imaginary unit. It is important to note that the window also depends on f, causing the width of the window to decrease with increasing frequency [18]. So, it can solve the problem of window function selection and overcome the disadvantages of fixed window width.

Since ST is established on the premise of the FT, the discrete S-transform (DST) can be obtained by FFT. Letting $\tau \to kT, f \to n/NT$, DST representations are available from (1) and (2) [19]:

$$\begin{cases} S\left[kT, \dfrac{n}{NT}\right] = \displaystyle\sum_{m=0}^{N-1} X\left[\frac{n+m}{NT}\right] e^{\left(\frac{-2\pi^2 m^2}{n^2} + \frac{j2\pi mk}{N}\right)}, (n \neq 0) \\ S\left[kT, 0\right] = \dfrac{1}{N} \displaystyle\sum_{m=0}^{N-1} x\left(\frac{m}{NT}\right), (n = 0) \end{cases} \tag{3}$$

where T is the sampling interval, N is the number of sampling points, n is the frequency parameter, $k, m, n = 0, 1, 2, \ldots, N-1$. $X\left[\frac{n+m}{NT}\right]$ is obtained by shifting the input signal $x(t)$ by discrete FFT.

Thus, the complex amplitude-time-frequency matrix of discrete signal can be obtained by (3). Notations $(N/2+1) =$ number of rows in the matrix S, which corresponds to the sampling frequency; $N =$ number of columns in the matrix S, which corresponds to the point of sampling time. When f_s is the actual sampling frequency, the frequency difference between two adjacent rows is:

$$\Delta f = \frac{f_s}{N} \tag{4}$$

B. BAGGING ENSEMBLE LEARNING ALGORITHM

Fault detection, diagnosis and protection usual use single machine learning algorithms, including SVM, RF and KNN. These single algorithms achieve encouraging results and have the ability to deal with most protection problems, by correctly discriminating useful information contained within the fault signals from the unwanted information including healthy signals or disturbing signals [6]. If the ensemble learning classification technology is further adopted, the accuracy of fault detection, diagnosis and protection will be improved [12]–[14]. Bagging is a famous representative of parallel ensemble learning algorithms. It trains different sample subsets with the given base classifiers, and then votes the results of each base classifier to get a strong classifier [20]–[22]. Bagging is based on bootstrap sampling with replacement. Namely, the bagging algorithm iteratively selects a certain number of training samples randomly with replacement from the original data set. And after randomly selecting sample, the sample is immediately put back to the original data set and for the next selection again. For a given set D containing p samples, r-round sampling is performed, and q data ($q \leq p$) are randomly selected per round, thereby forming r sampling subsets ($D_1, D_2, D_3, \ldots, D_r$). Base classifiers $h_g(x, D_r)$ for each of the r sample subsets are selected and trained, and then integrated into a strong classifier $H(x, D)$. Since the sample subsets are different, the base classifiers trained for each sample subset are also different. The sampling with replacement ensures that there are repeated samples in multiple sample subsets to avoid poor training results.

The voting scheme is commonly used to integrate multiple base classifiers, following the principle that the minority obeys the majority. The majority voting rule takes the labels classified by the most classifier as the labels of the samples to be classified. The Equation is (5):

$$H(x) = c_{\left(\arg\max\limits_{Z} \sum_{g=1}^{r} h_g^Z(x)\right)} \tag{5}$$

where $c_Z = \{c_1, c_2, \ldots, c_L\}$ is the labels set; $Z \in \{1, 2, \ldots, L\}$; L is the number of class labels, r is the number of base classifiers; $h_g^Z(x)$ is the output of h_g on the class label c_Z; $g = 1, 2, \ldots, r$.

If the number of votes (majority) obtained by multiple labels is the same, one of the labels is generally randomly selected as the final result. The process of bagging ensemble learning algorithm is implemented as shown in Fig. 1.

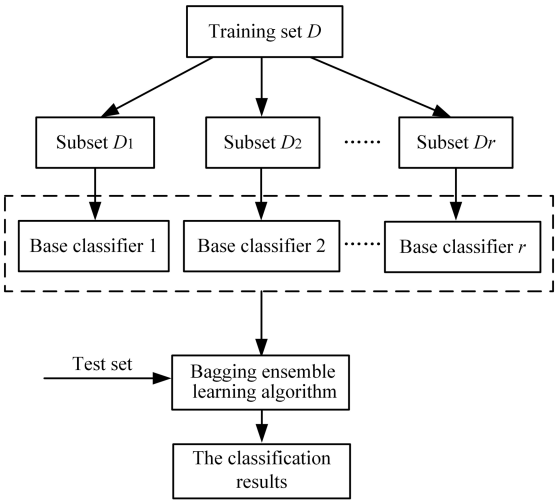

FIGURE 1. Process of bagging ensemble learning algorithm.

SVM, RF and KNN have achieved positive results in fault detection, diagnosis and protection of power system. Therefore, this paper first selects these three algorithms as the base classifiers of bagging algorithm and combines them into an ensemble classifier for fault discrimination of Powerformers.

III. FAULT FEATURES EXTRACTION

Powerformers are different from conventional generators in that their capacitance to ground is much larger than that of conventional generators, resulting in capacitance current is dozens of times of the conventional generator, so some weak information can be measured [6]. The information generated by the fault can be used to construct the feature vectors to reflect the operating state of Powerformers. The fault features generated by Powerformers is non-stationary. And the fault features in previous models ([6]–[8]) easily affected by fault resistance and fault locations. In order to solve this problem, ST is used to decompose the non-stationary fault signals (the zero-sequence current I_0) including the phase information and the absolutely-referenced frequency information in full time-frequency range, which can extract fault features more effectively. The transient energy, the comprehensive correlation coefficient and the zero-sequence active power of each Powerformer are extracted as fault features in the proposed protection scheme. And the contributions of this paper are emphasized in the Introduction.

A. TRANSIENT ENERGY EXTRACTED BY ST

The transient energy of the faulty Powerformer is much larger than that of the non-fault Powerformers, so the transient energy can be selected as the fault feature. The zero-sequence current of Powerformer is decomposed by the ST to obtain the complex amplitude-time-frequency matrix S. Then the energy of frequency band $A(i, l)$ (the i-th row in matrix A) of each Powerformer is calculated, and the maximum energy of frequency band is selected as the transient energy of the Powerformer. The following is the calculation process of transient energy extracted by ST.

The complex amplitude-time-frequency matrix S is obtained by ST. S_{il} is the element of the i-th row and l-column of the matrix S, whose real part is X and the imaginary part is Y correspond to the l-th time period at the i-th frequency. Its magnitude a_i^l is defined as:

$$\begin{cases} A_{il} = a_i^l = |S_{il}| * \Lambda \\ \Lambda = \text{sign}(\arctan\dfrac{Y}{X}) \end{cases} \tag{6}$$

where Λ represents the phase polarity at time-frequency, $i = 1, 2, 3, \ldots, N/2 + 1$; $l = 1, 2, 3, \ldots, N$.

All of A_{il} are calculated according to (6) to form the amplitude-time-frequency matrix A:

$$A = \begin{bmatrix} a_1^1 & \cdots & a_1^l & \cdots & a_1^N \\ \vdots & & \vdots & & \vdots \\ a_i^1 & \cdots & a_i^l & \cdots & a_i^N \\ \vdots & & \vdots & & \vdots \\ a_{\frac{N}{2}+1}^1 & & a_{\frac{N}{2}+1}^l & & a_{\frac{N}{2}+1}^N \end{bmatrix} \tag{7}$$

Fig. 2 (a) and (b) show the three-dimensional graphs of the amplitude-time-frequency matrix A of the faulty Powerformer and the non-fault Powerformer, respectively.

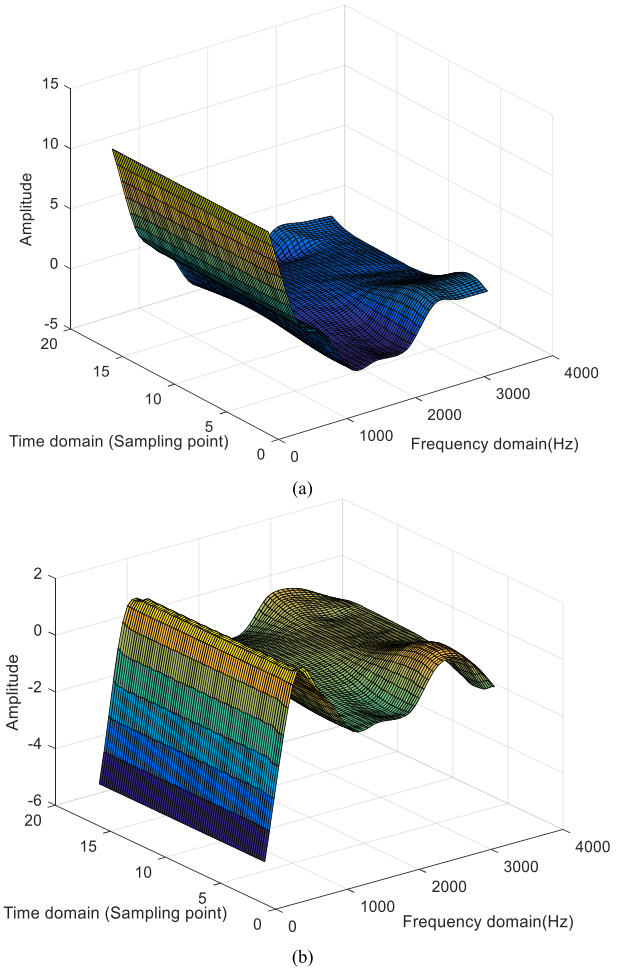

FIGURE 2. Three-dimensional graphs of the amplitude-time-frequency matrix *A*: (a) the faulty Powerformer; (b) the non-fault Powerformer.

It can be seen that the frequency bands of the former and the latter are significantly different.

Letting the transient energy of the Powerformer η be E_η, and the Equation is as follows:

$$\begin{cases} E_\eta(i) = \sum_{l=1}^{N} |A_{il}|^2 \\ E_\eta = \max(E_\eta(i)), \quad i = [1, \frac{N}{2} + 1] \end{cases} \tag{8}$$

where $E_\eta(i)$ is the energy of frequency band (the i-th row elements in matrix A), and E_η is the maximum value of $E_\eta(i)$ in matrix A.

In order to eliminate the discrepancies caused by the measurement at different scales, the transient energy can be normalized at the same proportional scale as:

$$e = \frac{E_\eta}{\sum_{\eta=1}^{J} E_\eta} \tag{9}$$

where J is the number of Powerformers connected in parallel in the system ($J \geq 3$). $\sum_{\eta=1}^{J} E_\eta$ is the sum of the transient energy of J Powerformers.

Therefore, in case of internal fault, the transient energy of the fault Powerformer is greater than that of the non-fault Powerformers, and their values range from 0 to 1. While the fault occurs in external system, the transient energy of all Powerformers are roughly equal, close to $1/J$. It can be used as the criterion for Powerformer protection scheme.

B. COMPREHENSIVE CORRELATION COEFFICIENT OF ST

In the process of modeling, voltage and current signals were extracted from the sensor, and all classifications of signals (including steady-state & transient components, fundamental & harmonic components, active & reactive components, fault components of each phase, sequence components) are taken as artificial features to establish the criterion. And then base on the correlation analysis, the correlation coefficient of the characteristic frequency band is selected for fault discrimination of Powerformers. In order to better reflect the difference between the amplitude-time-frequency matrixes of Powerformers, the correlation coefficient is defined. According to Section IV A, the frequency band $A(i, l)$ with the maximal energy is calculated. Then calculate $M = \arg\max_{i \in [1, N/2+1]} (E_\eta(i))$.

The M-th row of matrix A corresponds to the characteristic frequency band. This characteristic frequency band $A(M, l)$ is used as the dominant frequency vector for each Powerformer. Then the defined correlation coefficient is calculated as follows:

$$R_{\eta\beta} = \frac{\sum_{l=1}^{N} A_\eta(M, l) A_\beta(M, l)}{\sqrt{\sum_{l=1}^{N} A_\eta^2(M, l) \sum_{l=1}^{N} A_\beta^2(M, l)}} \tag{10}$$

where $R_{\eta\beta}$ represents the correlation coefficient between Powerformer η and Powerformer β. $A_\eta(M, l)$ and $A_\beta(M, l)$ are the dominant frequency vectors of Powerformer η and Powerformer β, respectively.

Since the inductive current cannot be abruptly changed at the initial stage of the fault, the fault current cannot be fully compensated by Petersen coil. Therefore, in the resonant grounding system, the characteristics of the zero-sequence current component at the initial stage of the fault are mainly determined by the transient capacitor current component. At this time, the magnitude and direction of the transient zero-sequence current component of the faulty Powerformer and of the non-fault Powerformers are quite different, while the difference between that of the non-fault Powerformers is relatively small. As a result, the correlation coefficient between the faulty Powerformer and the non-fault Powerformer is close to -1, and the correlation coefficient among the non-fault Powerformers is close to 1. In the high-resistance grounding system, the current component of the faulty Powerformer and of non-fault Powerformer is at a certain angle difference, but still meet the above correlation coefficient relationship.

In order to more intuitively reflect the differences of Powerformers, this paper defines the comprehensive correlation coefficient of Powerformer η as follows:

$$\rho = \frac{1}{J-1}\left(\sum_{\beta=1}^{J} R_{\eta\beta} - 1\right) = \frac{1}{J-1} \sum_{\beta=1, \beta\neq\eta}^{J} R_{\eta\beta} \tag{11}$$

where $\sum_{\beta=1, \beta\neq\eta}^{J} R_{\eta\beta}$ is the sum of the correlation coefficients between Powerformer η and other Powerformers in the system. It can ensure that the correlation coefficient between the Powerformer η and other Powerformers in the system can be effectively calculated.

After a stator SLG fault occurs in power system, the comprehensive correlation coefficient of the faulty Powerformer is close to -1, and that of the non-fault Powerformers is close to $1 - 2/(J-1)$. It can be used as the criterion for Powerformer protection scheme.

C. ZERO-SEQUENCE ACTIVE POWER

The zero-sequence active power is the integral average of zero sequence current and zero sequence voltage in a power frequency cycle (T_1). The expression is as follows:

$$\begin{cases} \Delta P_\eta = \frac{1}{T} \int_t^{t+T_1} \Delta U_0(t) \Delta I_{0\eta}(t) dt \\ \Delta U_0(t) = U_0(t) - U_0(t - 2T_1) \\ \Delta I_{0\eta}(t) = I_{0\eta}(t) - I_{0\eta}(t - 2T_1) \end{cases} \tag{12}$$

where, ΔP_η, $\Delta U_0(t)$ and $\Delta I_{0\eta}(t)$ are the average active power fault component, the zero-sequence voltage fault component and the zero-sequence current fault component in the terminal of Powerformer η, respectively.

It can be known from (12) that the difference of ΔP_η in Powerformers connected in parallel is mainly reflected

by $\Delta I_{0\eta}(t)$. However, the magnitude of zero-sequence current of the faulty Powerformer is greater than the sum of non-fault Powerformers, and the direction of zero-sequence current of the former is different from that of the latter.

Then, the zero-sequence active power of Powerformer η can be defined:

$$\lambda = \frac{\Delta P_\eta}{\sum_{\eta=1}^{J} \left|\Delta P_\eta\right|} \tag{13}$$

where $\sum_{\eta=1}^{J} \left|\Delta P_\eta\right|$ is the sum of the absolute value of zero-sequence active power of J Powerformers. Therefore, it can be known that the value of the zero-sequence active power of the faulty Powerformer is in the range of 0 to 1, while the value of zero-sequence active power of the non-fault Powerformers is in the range of -1 to 0. It can also be used as the criterion for Powerformer protection scheme.

D. EXTRACTION PROCESS OF THE FEATURE VECTORS

The above three fault features can constitute a feature vector $x = (e, \rho, \lambda)$, which represents the current operating state of Powerformers. For each fault, each Powerformer in the system can obtain a feature vector, and a data set of feature vectors can be formed. The extraction process of the feature vectors is shown in Fig. 3. Where K is the number of feature vector samples, x_K is the K-th feature vector sample.

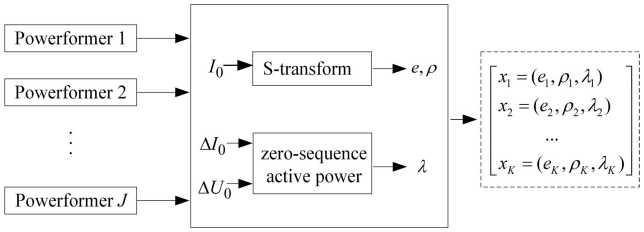

FIGURE 3. The extraction process of the feature vectors.

IV. PROTECTION PRINCIPLE WITH S-TRANSFORM AND BAGGING ENSEMBLE LEARNING FOR POWERFORMERS

The proposed protection scheme is suitable for a system with three or more bus-connected Powerformers ($J \geq 3$). And as long as the parameters of the parallel Powerformers are similar, the proposed scheme is suitable for various types of Powerformers. Fig. 4 shows the system model for J Powerformers connected in parallel. The fault resistance is set from 5 to 8000 Ω, and the neutral point of Powerformers is grounded by high-resistance or reactance, which helps to form training and test data sets for the bagging ensemble learning algorithm. The following five steps illustrate the principle of the stator SLG fault protection scheme for Powerformers.

Step1: The zero-sequence voltage of the system is measured from the voltage transformer (VT) connected to the busbar to determine whether a SLG fault occurs in the system.

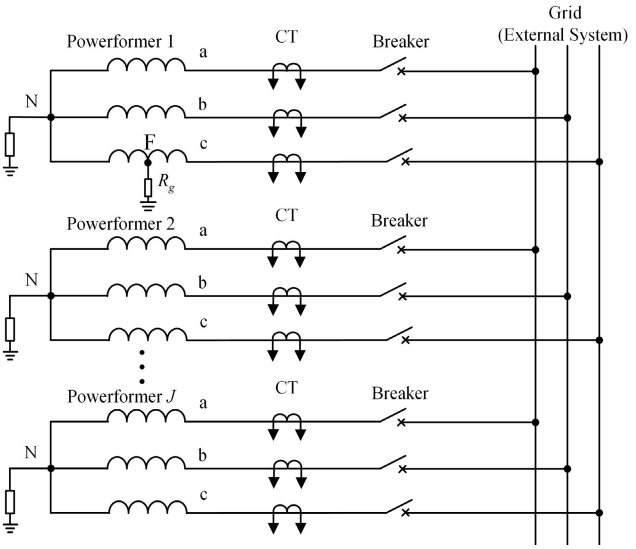

FIGURE 4. System model for Powerformers connected in parallel.

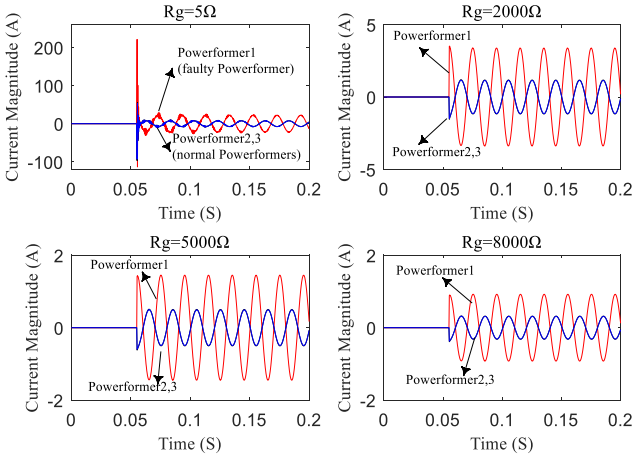

FIGURE 5. Zero-sequence current waveform of Powerformers. Note: a parallel system with three Powerformers is taken as an example (fault started at 0.055s).

Step2: After detected the SLG fault in the system, the zero-sequence voltage and the zero-sequence current of Powerformers are sampled. Fig. 5 shows the zero-sequence current waveform of three Powerformers when stator SLG faults occur in Powerformer 1 (This paper uses the parameter setting in the ATP-EMTP simulation software to set the switch to close at 0.055s for controlling the level of current). The direction of the zero-sequence current of the faulty Powerformer and the normal Powerformers is almost opposite, and the magnitude of the zero-sequence current is greatly different.

Step3: The zero-sequence current in the first quarter of the power frequency cycle ($T_1/4$) after the fault is decomposed by ST. And all the amplitude-time-frequency elements are calculated according to (6) and (7) to form the amplitude-time-frequency matrix A. Then the ST transient energy e, the comprehensive correlation coefficient ρ and the zero-sequence active power λ are calculated according to (9), (11) and (13), respectively.

Step4: According to the Fig. 3, the above three fault features obtained in Step3 constitute the data set of fault feature vectors.

Step5: The final step is utilizing bagging ensemble learning algorithm for fault protection. In this scheme, the data set is divided into training set (70% of the data) and test set (the rest 30% of the data), and different base classifiers SVM, RF and KNN are used for training, then the output results are voted to get the final labels. Finally, the fault protection result is output, that is, the operating state of Powerformers is judged: fault (1), non-fault (0), and external fault (2).

The proposed scheme generates different testing data sets considering the effects of measurement noise to test the performance of the bagging ensemble learning algorithm. Fig. 6 shows the complete flow chart of the proposed fault protection scheme.

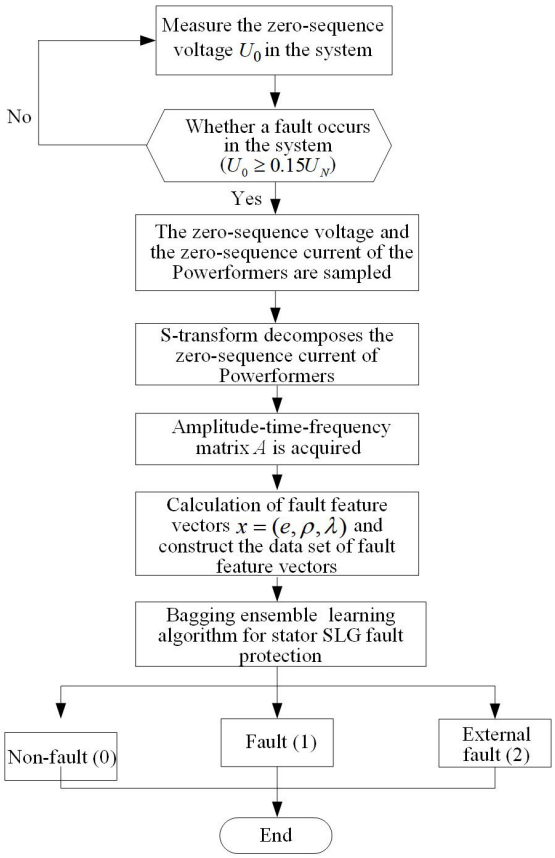

FIGURE 6. Flow chart of the stator SLG fault protection scheme.

V. SIMULATION ANALYSIS

A. SIMULATION MODEL

The simulation model of the stator SLG fault of Powerformer is built by ATP-EMTP. Three Powerformers connected in parallel are directly connected to the external system of the grid is taken as an example. The equivalent circuit of capacitance of the Powerformer winding is shown in Fig. 7. One portion αC_g of the total capacitance to ground of the winding C_g can

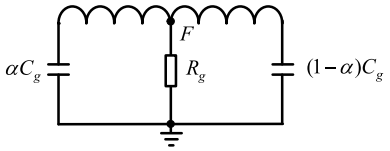

FIGURE 7. Equivalent circuit of capacitance of the Powerformer winding.

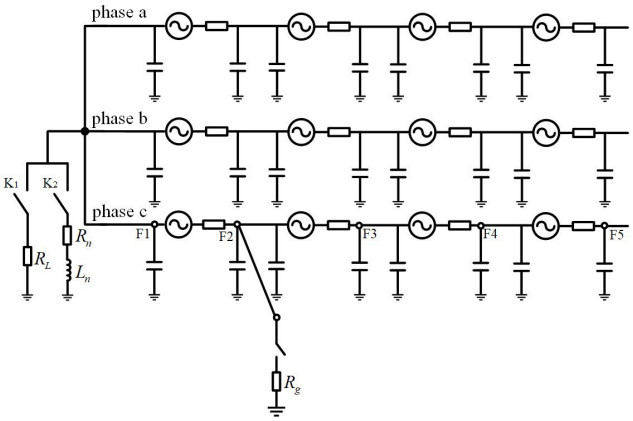

FIGURE 8. Stator winding model of Powerformer 1 and an internal stator SLG fault at 25% of phase c.

be associated with the voltage at the generator neutral of the phase winding while the rest $(1-\alpha)C_g$, can be associated with the voltage at the generator terminal of the winding [23], [24]. In addition, the stator winding model of each Powerformer is established, and each phase of the stator winding is divided into 4 units. The electromotive force and resistance of the stator winding are equally divided into each unit circuit, as shown in Fig. 8. An internal stator SLG fault occurs at the stator winding in phase c of Powerformer 1. Where K_1 and K_2 are used to switch the neutral grounding methods of Powerformer: K_1 closure represents the high-resistance grounding, K_2 closure represents the reactance grounding.

The Powerformers have the following characteristics:

(1) The rated capacity, the rated voltage, the rated frequency, the winding capacitance (C_{g1}, C_{g2}, C_{g3}) to ground per phase of Powerformer1-3, and the capacitance (C_t) to ground per phase of external system are the same as those used in [8].
(2) The inception angle is 0°;
(3) The inductance L_n is 1838mH;
(4) The damping resistance R_n is 57Ω;
(5) The neutral grounding resistance R_L is 1900Ω;
(6) Grounding fault starts at 0.055s;
(7) The following faults were simulated:

a. Fault resistance R_g: 5, 100, 500, 750, 1000, . . . , 7500, 7750, 8000 Ω;

b. Internal SLG fault when 0%, 25%, 50%, 75%, 100% of the stator winding are grounded (Fig. 8 is marked with "F");

c. Different external faults;

d. The neutral grounding methods: high-resistance grounding or reactance grounding.

TABLE 1. Simulation results of feature vectors of all Powerformers.

Neutral grounding methods	R_g / Ω	α	Powerformer 1			Powerformer 2			Powerformer 3		
			e	ρ	λ	e	ρ	λ	e	ρ	λ
high -resistance grounding	5	0%	0.6999	-0.9963	0.5880	0.1557	0.0018	-0.2066	0.1443	0.0019	-0.2055
	100	25%	0.7801	-1.0000	0.5846	0.1114	0.0000	-0.2082	0.1086	0.0000	-0.2072
	500	50%	0.7787	-1.0000	0.5811	0.1125	0.0000	-0.2098	0.1088	0.0000	-0.2091
	...	...	...	...	...	...	...	...	...	...	...
	7500	75%	0.7768	-1.0000	0.5778	0.1137	0.0000	-0.2112	0.1095	0.0000	-0.2109
	7750	100%	0.7768	-1.0000	0.5778	0.1137	0.0000	-0.2112	0.1095	0.0000	-0.2109
	8000	--	0.3291	1.0000	-0.3332	0.3418	1.0000	-0.3337	0.3291	1.0000	-0.3332
reactance grounding	5	0%	0.6999	-0.9960	0.6567	0.1559	0.0019	-0.1726	0.1443	0.0020	-0.1707
	100	25%	0.7300	-1.0000	0.6684	0.1354	0.0000	-0.1671	0.1346	0.0000	-0.1646
	500	50%	0.7398	-1.0000	0.6639	0.1306	0.0000	-0.1689	0.1296	0.0000	-0.1672
	...	...	...	...	...	...	...	...	...	...	...
	7500	75%	0.7461	-1.0000	0.6504	0.1277	0.0000	-0.1750	0.1261	0.0000	-0.1746
	7750	100%	0.7461	-1.0000	0.6503	0.1277	0.0000	-0.1750	0.1261	0.0000	-0.1746
	8000	--	0.3320	1.0000	-0.3331	0.3361	1.0000	-0.3338	0.3320	1.0000	-0.3331

Note: only part of the data is listed, where "--" represents SLG fault occurring in external system.

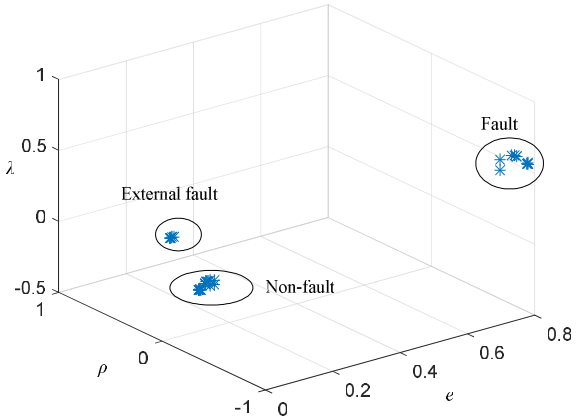

FIGURE 9. Part of sample data mapped into three-dimensional space.

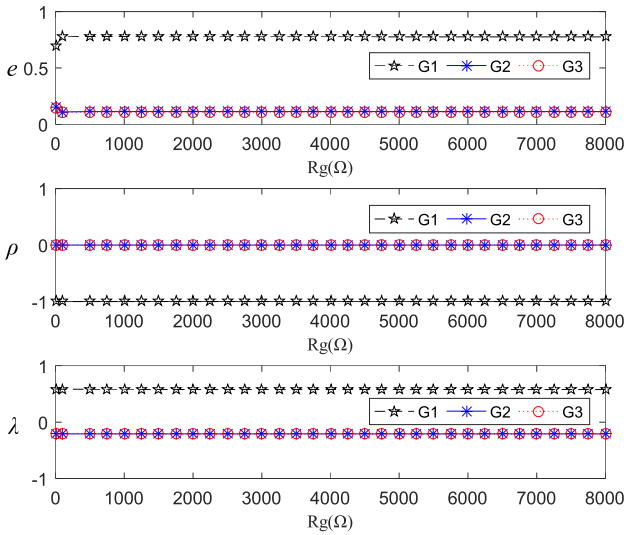

FIGURE 10. Effection of fault resistance on the valves of fault features. Note: G1, G2 and G3 represent Powerformer 1, 2 and 3 respectively.

B. SIMULATION DATA RESULTS

This paper changes the fault conditions by changing the neutral grounding methods, the fault resistance and the fault location, thereby increasing the diversity of samples to evaluate the detection efficiency. The above fault conditions were simulated, and the ST transient energy e, the comprehensive correlation coefficients ρ and the zero-sequence active power λ were calculated. The simulation data of faults under different conditions were obtained as shown in Table 1. Due to limited space, only part of the data is listed, where "–" represents SLG fault occurring in external system. Powerformer protection is regarded as a classification problem in this paper. As shown in Fig. 9, the data set are projected in multidimensional space, and the dimension of the space is the number of features. The distribution of the samples in each dimension can reflect the impact of features in the protection results. If the selected features make the relative distance between the classes larger (samples in the same class are highly similar to each other; and separation signals from different classes have low similarity to each other), the selected features contribute more to the protection scheme.

TABLE 2. Classification results of the proposed scheme.

Operating state	Samples (357)	Classification results			Accuracy
		Fault	Non-fault	External fault	
Fault	95	95	0	0	100%
Non-fault	203	0	203	0	100%
External fault	59	0	0	59	100%

C. EFFECTION OF FAULT RESISTANCE

The fault current is very weak when the fault resistance is high. Generally, when the fault resistance reaches about 5000 Ω, the traditional over-current relay cannot detect the fault correctly. Therefore, this paper needs to consider the effect of fault resistance on the values of fault features. Various conditions of fault resistance from 5-8000 Ω were verified.

TABLE 3. Performance of classifiers for the test set under different noise levels.

Classifier	30dB/20dB			15dB			10dB			5dB		
	Accuracy	Recall	F1-score	Accuracy	Recall	F1-score	Accuracy	Recall	F1-score	Accuracy	Recall	F1-score
Bagging	**100%**	**100%**	**100%**	**100%**	**100%**	**100%**	**95.80%**	**96.84%**	**96.32%**	**82.35%**	**84.21%**	**83.27%**
SVM	100%	100%	100%	99.44%	100%	99.72%	94.40%	95.79%	95.09%	80.95%	84.21%	82.55%
RF	100%	100%	100%	99.72%	100%	99.86%	92.44%	93.68%	93.06%	76.75%	81.05%	78.84%
KNN	100%	100%	100%	94.96%	95.79%	95.37%	94.96%	95.79%	95.37%	77.31%	71.58%	74.33%

Fig. 10 shows the relationship between fault resistance and the values of fault features e, ρ, λ ($\alpha = 25\%$, SLG fault at Powerformer 1). With the increase of the fault resistance, the values of three fault features are almost unchanged. Even if the R_g reaches 8000 Ω, the values of e, ρ, λ of non-fault Powerformers and faulty Powerformer are still significantly different. It can be inferred that fault resistance has no effect on the protection scheme proposed in this paper.

D. EFFECTION OF FAULT LOCATIONS AND EXTERNAL FAULTS

In the previous models [6]–[8], different fault locations caused significant changes in the values of fault features. Considering this effect, stator SLG faults at phase c ($R_g = 5\Omega$, $\alpha = 25\%, 50\%, 75\%, 100\%$) of Powerformer 1 and faults at external system were verified. The relationship between the fault locations and the values of the fault features is shown in Fig. 11. As can be observed, in the case of internal fault, the values of fault features did not change with the fault locations, so the fault features can easily distinguish the faulty Powerformer from the healthy Powerformers. When a fault occurs in an external system, the values of fault features of each Powerformer are almost the same.

E. FAULT DETECTION AND CLASSIFICATION PROBLEM

A total of 1188 sample data were obtained from the simulation, of which 831 are training samples and 357 are test samples. After the bagging ensemble learning fault detection model is trained, the test samples are used as input to the classifier for fault detection. The classification results are shown in Table 2.

Table 2 shows the proposed scheme is able to distinguish faulty Powerformer from non-fault Powerformers with 100% accuracy, as well as to identify internal faults and external faults. When the internal fault occurs, the data obtained from Powerformer 1 indicates a fault, while the data obtained from Powerformer 2 and 3 indicate the normal operation on the contrary. When a fault occurs in the external system, the data of three Powerformers indicates the external fault. From the above analysis, it can be inferred that the proposed scheme is independent of the neutral grounding methods and fault resistance.

F. FAULT PROTECTION IN NOISY ENVIRONMENT

The proposed scheme added additive white Gaussian noise (AWGN) to the zero-sequence current signals measured from the Powerformer terminal to test the efficacy of the trained bagging ensemble learning algorithm. In the presence of 30, 20, 15, 10dB signal-to-noise ratio (SNRs), the proposed scheme is compared with SVM, RF and KNN.

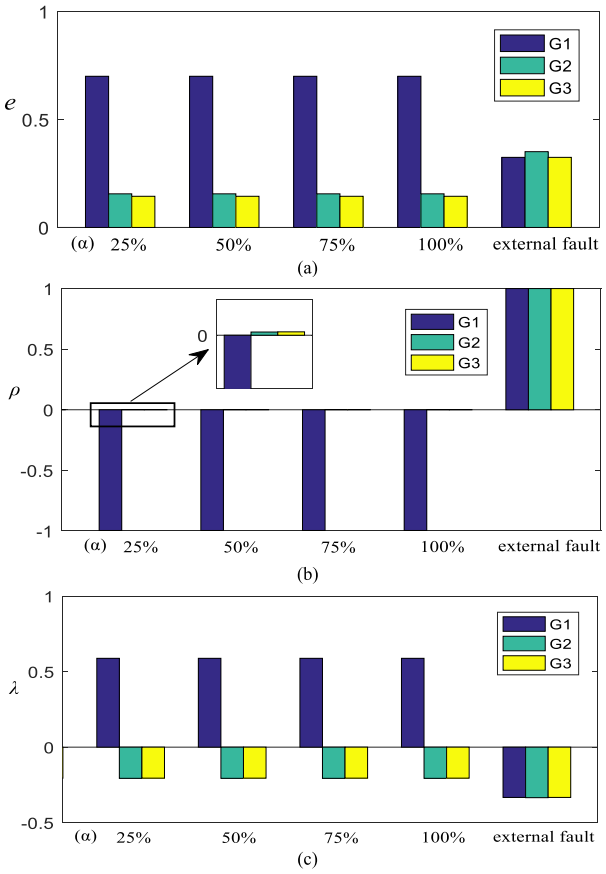

FIGURE 11. Relationship between fault locations and the values of fault features. (a) the values of e; (b) the values of ρ; (c)the values of λ. Note: G1, G2 and G3 represent Powerformer 1, 2 and 3 respectively.

Table 3 shows the comparison of fault protection performance between bagging ensemble learning algorithm and single algorithms under different noise levels. Three evaluation indexes of *accuracy*, *recall* and *F1-score* [25] are used to evaluate the fault protection technology. According to Table 3, bagging ensemble learning algorithm is superior to the single algorithm in the three evaluation indexes mentioned above. And the stronger the noise intensity is, the better the performance of the proposed algorithm is.

VI. CONCLUSIONS

This paper proposed a novel stator SLG fault protection scheme for Powerformers. The proposed scheme decom-

poses the zero-sequence current signals measured from Powerformer terminal and extracts feature vectors employing ST. Then, the feature vectors are used as inputs to bagging ensemble learning algorithm to detect faults under different conditions. Simulation results demonstrate the effectiveness of the proposed scheme on detecting the SLG faults in the system of parallel connection of Powerformers. Its specific merits are as follows:

(1) The bagging ensemble learning algorithm trains SVM RF and KNN as the base classifiers, and then votes the results of each base classifier to get a strong classifier. It improves the reliability of the protection scheme.

(2) This protection scheme does not need to set the threshold value. In addition, the technique is independent of the neutral grounding methods and fault resistance, and can detect in which Powerformer a stator SLG fault is occurring even if the fault resistance is at 8000 Ω.

(3) Under different fault conditions, the novel scheme can distinguish internal faults from external faults reliably. Besides, the proposed technique shows better generalization ability and noise-tolerant ability than SVM, RF and KNN techniques in detecting faults.

REFERENCES

[1] T. Nengling and J. Stenzel, "Differential protection based on zero-sequence voltages for generator stator ground fault," *IEEE Trans. Power Del.*, vol. 22, no. 1, pp. 116–121, Jan. 2007.

[2] Y. Gao, X. Lin, Q. Tian, and P. Liu, "Novel identification method of stator single phase-to-ground fault for cable-wound generators," *IEEE Trans. Energy Convers.*, vol. 23, no. 2, pp. 349–357, Jun. 2008.

[3] N. Safari-Shad, R. Franklin, A. Negahdari, and H. A. Toliyat, "Adaptive 100% injection-based generator stator ground fault protection with real-time fault location capability," *IEEE Trans. Power Del.*, vol. 33, no. 5, pp. 2364–2372, Oct. 2018.

[4] K. Al Jaafari, A. Negahdari, H. A. Toliyat, N. Safari-Shad, and R. Franklin, "Modeling and experimental verification of a 100% stator ground fault protection based on adaptive third-harmonic differential voltage scheme for synchronous generators," *IEEE Trans. Ind. Appl.*, vol. 53, no. 4, pp. 3379–3386, Jul./Aug. 2017.

[5] N. Safari-Shad and R. Franklin, "Adaptive 100% stator ground fault protection based on third-harmonic differential voltage scheme," *IEEE Trans. Power Del.*, vol. 31, no. 4, pp. 1429–1436, Aug. 2016.

[6] Y. Y. Wang, X. J. Zeng, J. B. Jian, Z. Y. Dong, Z. W. Li, and Y. Huang, "Studies on the stator single-phase-to-ground fault protection for a high-voltage cable-wound generator," *IEEE Trans. Energy Convers.*, vol. 28, no. 2, pp. 344–352, Jun. 2013.

[7] Y. Y. Wang, X. J. Zeng, Z. Y. Dong, Y. Xu, J. Yuan, and Y. Huang, "Stator single-phase-to-ground fault protection for bus-connected powerformers based on hierarchical clustering algorithm," *IEEE Trans. Energy Convers.*, vol. 28, no. 4, pp. 991–998, Dec. 2013.

[8] Y. Wang, X. Zeng, Z. Dong, and Y. Huang, "Novel protection scheme of stator single-phase-to-ground fault for powerformers," *Int. J. Electr. Power Energy Syst.*, vol. 53, pp. 321–328, Dec. 2013.

[9] H. Livani and C. Y. Evrenosoglu, "A machine learning and wavelet-based fault location method for hybrid transmission lines," *IEEE Trans. Smart Grid*, vol. 5, no. 1, pp. 51–59, Jan. 2014.

[10] S. R. Samantaray, "Ensemble decision trees for high impedance fault detection in power distribution network," *Int. J. Electr. Power Energy Syst.*, vol. 43, no. 1, pp. 1048–1055, Dec. 2012.

[11] S. R. Madeti and S. N. Singh, "Modeling of PV system based on experimental data for fault detection using kNN method," *Sol. Energy*, vol. 173, pp. 139–151, Oct. 2018.

[12] Y. Wang, K. Zhu, M. Sun, and Y. Deng, "An ensemble learning approach for fault diagnosis in self-organizing heterogeneous networks," *IEEE Access*, vol. 7, pp. 125662–125675, 2019.

[13] G. I. Webb and Z. Zheng, "Multistrategy ensemble learning: Reducing error by combining ensemble learning techniques," *IEEE Trans. Knowl. Data Eng.*, vol. 16, no. 8, pp. 980–991, Aug. 2004.

[14] M. Z. Ali, M. N. S. K. Shabbir, X. Liang, Y. Zhang, and T. Hu, "Machine learning-based fault diagnosis for single- and multi-faults in induction motors using measured stator currents and vibration signals," *IEEE Trans. Ind. Appl.*, vol. 55, no. 3, pp. 2378–2391, May/Jun. 2019.

[15] P. K. Mishra, A. Yadav, and M. Pazoki, "A novel fault classification scheme for series capacitor compensated transmission line based on bagged tree ensemble classifier," *IEEE Access*, vol. 6, pp. 27373–27382, 2018.

[16] A. Ghaderi, H. L. Ginn, and H. A. Mohammadpour, "High impedance fault detection: A review," *Electr. Power Syst. Res.*, vol. 143, pp. 376–388, Feb. 2017.

[17] M. Shafiullah and M. A. Abido, "S-transform based FFNN approach for distribution grids fault detection and classification," *IEEE Access*, vol. 6, pp. 8080–8088, 2018.

[18] T. Zhong, S. Zhang, G. Cai, Y. Li, B. Yang, and Y. Chen, "Power quality disturbance recognition based on multiresolution S-Transform and decision tree," *IEEE Access*, vol. 7, pp. 88380–88392, 2019.

[19] R. G. Stockwell, L. Mansinha, and R. P. Lowe, "Localization of the complex spectrum: The s transform," *IEEE Trans. Signal Process.*, vol. 44, no. 4, pp. 998–1001, Apr. 1996.

[20] B. Wang and J. Pineau, "Online bagging and boosting for imbalanced data streams," *IEEE Trans. Knowl. Data Eng.*, vol. 28, no. 12, pp. 3353–3366, Dec. 2016.

[21] Y. Lv, S. Peng, Y. Yuan, C. Wang, P. Yin, J. Liu, and C. Wang, "A classifier using online bagging ensemble method for big data stream learning," *Tsinghua Sci. Technol.*, vol. 24, no. 4, pp. 379–388, Aug. 2019.

[22] X. Li, T. Shi, P. Li, and W. Zhou, "Application of bagging ensemble classifier based on genetic algorithm in the text classification of railway fault hazards," in *Proc. 2nd Int. Conf. Artif. Intell. Big Data (ICAIBD)*, Chengdu, China, May 2019, pp. 286–290.

[23] Q. Tian, Z. Liu, and X. Lin, "A new approach to winding capacitance dividing method for the generator with considerable winding distributed capacitance," in *Proc. 3rd Int. Conf. Electr. Utility Deregulation Restructuring Power Technol.*, Nanjing, China, Apr. 2008, pp. 1672–1677.

[24] Q. Tian, X. Lin, and P. Liu, "A novel self-adaptive compensated differential protection design suitable for the generator with considerable winding distributed capacitance," *IEEE Trans. Power Del.*, vol. 22, no. 2, pp. 836–842, Apr. 2007.

[25] J. Sun, J. Lang, H. Fujita, and H. Li, "Imbalanced enterprise credit evaluation with DTE-SBD: Decision tree ensemble based on SMOTE and bagging with differentiated sampling rates," *Inf. Sci.*, vol. 425, pp. 76–91, Jan. 2018.

YUANYUAN WANG (Member, IEEE) received the B.S. and M.Sc. degrees in electrical engineering from the Changsha University of Science and Technology, China, in 2004 and 2007, respectively, the Ph.D. degree in electrical engineering from the College of Electrical Engineering, Guangxi University, Guangxi, China, in 2012.

She is currently an Associate Professor with the College of Electrical and Information Engineering, Changsha University of Science and Technology. Her research interest includes power system protection and control.

YONGSHENG GUO received the B.S. degree in electrical engineering and its automation from the Changsha University of Science and Technology, Changsha, China, in 2018, where he is currently pursuing the M.S. degree in electrical engineering with the School of Electrical and Information Engineering.

His research interest includes power system protection and control.

XIANGJUN ZENG (Senior Member, IEEE) received the B.S. degree in electrical engineering from Hunan University, Changsha, China, in 1993, the M.S. degree in electrical engineering from Wuhan University, Wuhan, China, in 1996, and the Ph.D. degree in electrical engineering from the Huazhong University of Science and Technology, Wuhan, in 2001.

He was a Postdoctoral Fellow with Xuji Relay Company and Hong Kong Polytechnic University and a Visiting Professor with Nanyang Technological University, Singapore. He is currently a Professor and the Dean of the School of Electrical and Information Engineering, Changsha University of Science and Technology, Changsha. His research focuses on real-time computer applications in power systems control and protection.

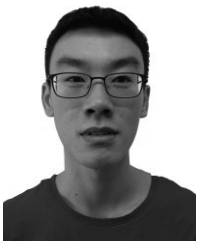

JUN CHEN received the B.S. degree in electrical engineering and its automation from the Hunan Institute of Technology, Hengyang, China, in 2018. He is currently pursuing the M.S. degree in electrical engineering with the School of Electrical and Information Engineering, Changsha University of Science and Technology, Changsha, China.

His research interest includes power system protection and control.

YANG KONG received the B.S. degree in electrical engineering and its automation from the Changsha University of Science and Technology, Changsha, China, in 2018, where he is currently pursuing the M.S. degree in electrical engineering with the School of Electrical and Information Engineering.

His research interest includes power system protection and control.

SHANFENG SUN received the B.S. degree in automobile support engineering from the Changsha University of Science and Technology, Changsha, China, in 2018, where he is currently pursuing the M.S. degree in electrical engineering with the School of Electrical and Information Engineering.

His research interest includes power system protection and control.